

QUANTITATIVE INTERPRETATION OF WITHIN-OUTCROP VARIATION IN METAMORPHIC ASSEMBLAGE IN STAUROLITE-KYANITE-GRADE METAPELITES, BALTIMORE, MARYLAND

HELEN M. LANG

Department of Geology and Geography, West Virginia University, Morgantown, West Virginia 26506, U.S.A.

ABSTRACT

Two metamorphic mineral assemblages, a staurolite (St) assemblage consisting of staurolite, garnet, biotite, quartz, muscovite, plagioclase, ilmenite and magnetite, and a staurolite - kyanite (St-Ky) assemblage consisting of kyanite, staurolite, garnet, biotite, quartz, muscovite, plagioclase, ilmenite, rutile and pyrrhotite, are randomly distributed along a 0.5-km-long exposure at the Hunt Valley Mall, north of Baltimore, Maryland. St and St-Ky assemblages equilibrated at the same temperature and total pressure. Intersections of adjusted solid-solid equilibria applicable to St-Ky assemblages yield estimated temperature and total pressure of approximately 590°C and 6.1 kilobars. Projections suggest that St assemblages equilibrated at higher $X(\text{H}_2\text{O})$ than St-Ky assemblages. The absence of mass-balance relationships between any St and St-Ky assemblages without excess rutile in the St assemblage shows that the two assemblages are related at least in part by a difference in bulk composition, perhaps different FeO content. Consideration of pressure - temperature, temperature - $X(\text{CO}_2)$ and $f(\text{O}_2) - f(\text{S}_2)$ phase relations among minerals in St and St-Ky assemblages suggests that they also equilibrated with metamorphic fluids of different composition. A provisional estimate of $X(\text{H}_2\text{O}) = 0.5$ for the metamorphic fluid in equilibrium with the St-Ky assemblage was derived from a GEØ-CALC T - $X(\text{CO}_2)$ diagram. St assemblages seem to have equilibrated with a metamorphic fluid that was more H_2O -rich with similar $f(\text{O}_2)$ and lower $f(\text{S}_2)$ than that with which St-Ky assemblages equilibrated.

Keywords: metapelites, mass balance, staurolite, kyanite, fluid composition, thermobarometry, Baltimore, Maryland.

SOMMAIRE

Deux assemblages de minéraux métamorphiques, un à staurolite (St) contenant staurolite, grenat, biotite, quartz, muscovite, plagioclase, ilménite et magnetite, et l'autre à staurolite - kyanite (St-Ky), contenant kyanite, staurolite, grenat, biotite, quartz, muscovite, plagioclase, ilménite, rutile et pyrrhotite, sont aléatoires dans leur distribution le long d'un affleurement de 0.5 km à Hunt Valley Mall, au nord de Baltimore, au Maryland. Les

assemblages St et St-Ky ont atteint l'équilibre aux mêmes conditions de température et de pression. Les intersections des équilibres solide-solide appropriés pour des exemples de l'assemblage St-Ky indiquent environ 590°C et 6.1 kilobars. Des projections semblables pour les exemples de l'assemblage St indiqueraient une valeur de $X(\text{H}_2\text{O})$ plus élevée que pour St-Ky. L'absence des relations d'équivalence des masses entre des assemblages St et St-Ky sans un excédent de rutile dans l'assemblage St montre que les deux assemblages sont liés, au moins en partie, par une différence en composition globale, peut être une différence en concentration de FeO. D'après une analyse des relations des minéraux des deux assemblages en termes de pression - température, température - $X(\text{CO}_2)$, et $f(\text{O}_2) - f(\text{S}_2)$, il semble de plus que la phase fluide qui a participé à l'équilibre dans les deux assemblages ait été différente. Une valeur provisoire pour $X(\text{H}_2\text{O})$ de 0.5 pour la phase fluide dans l'assemblage St-Ky résulte du diagramme T - $X(\text{CO}_2)$ calculé selon GEØ-CALC. Par contre, l'assemblage St semble avoir équilibré avec une phase fluide plus riche en eau, à une valeur de $f(\text{O}_2)$ semblable, mais à une valeur de $f(\text{S}_2)$ inférieure que pour l'assemblage St-Ky.

(Traduit par la Rédaction)

Mots-clés: métapélites, équivalence des masses, staurolite, kyanite, composition de la phase fluide, thermobarométrie, Baltimore, Maryland.

INTRODUCTION

Considerable progress has been made in recent decades in estimating metamorphic conditions from mineral assemblages and mineral compositions. However, there is still no routine way to distinguish between the effects of variation in intensive parameters and those due to variation in bulk composition. Distinction of these two types of effects requires recognition of reaction or mass-balance relationships between pairs of assemblages. A reaction relationship is indicated by crossing tie-lines on a thermodynamically valid graphical projection (Greenwood 1975). Because graphical representations of relationships in complex multi-

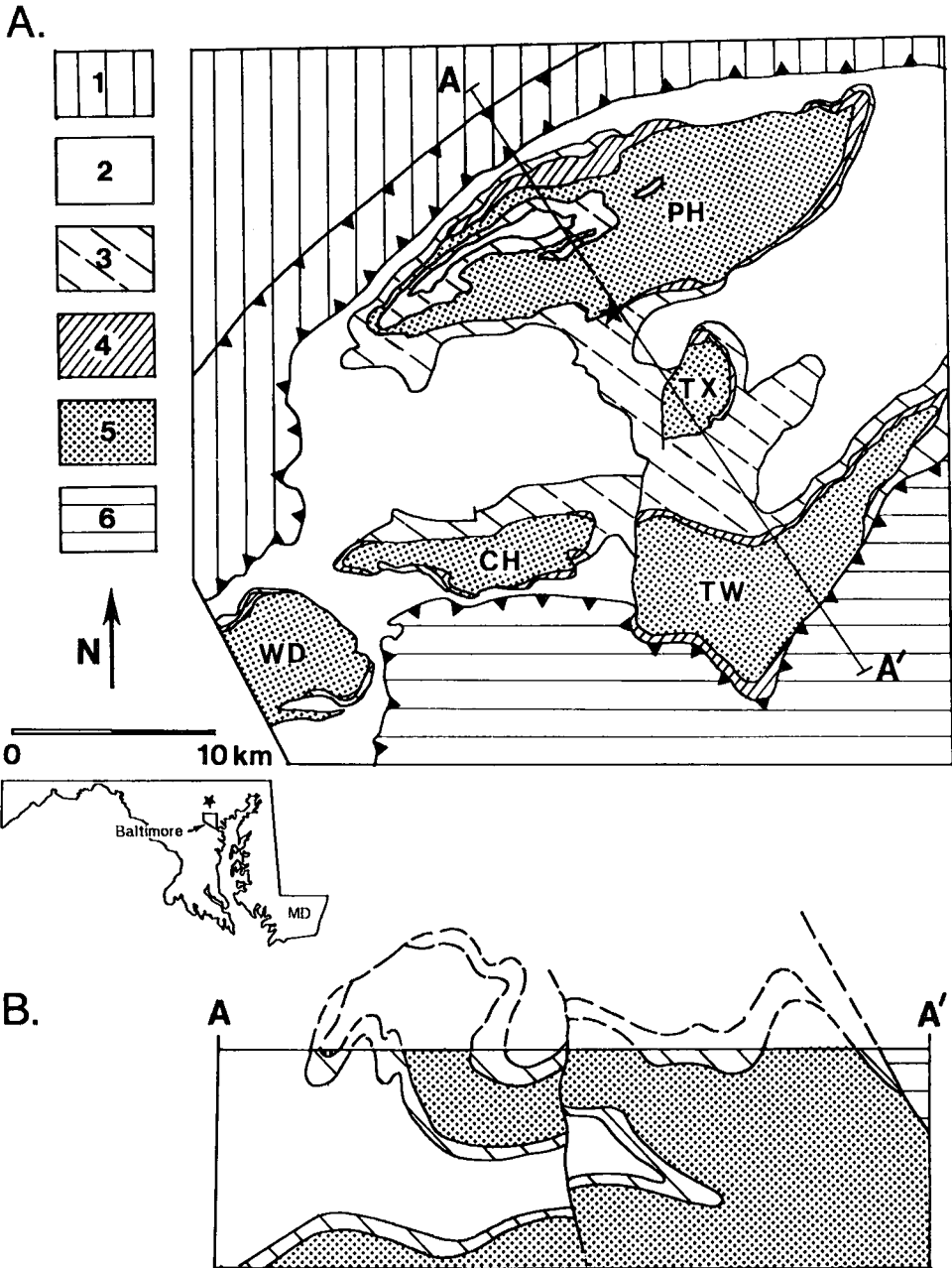


FIG. 1. A. Generalized geological map of Baltimore County and adjacent areas (after Crowley *et al.* 1976, Muller *et al.* 1989). Units: 1 Low- to medium-grade metasediments of the western Piedmont, 2 Loch Raven Formation, mainly pelitic schist, 3 Cocksylville Marble, 4 Setters Formation, quartzite and pelitic schist, 5 Baltimore Gneiss, felsic basement gneiss, 6 Baltimore Mafic Complex, island-arc complex that collided with the Baltimore Gneiss Terrane (units 2-5) during the Taconic Orogeny (at approximately 470 Ma). Anticlines in which the Baltimore Gneiss is exposed are labeled PH (Phoenix), TX (Texas), TW (Towson), CH (Chattolance), and WD (Woodstock). The line labeled A-A' shows the approximate location of the schematic cross-section shown in B. The location of the Hunt Valley Mall exposure is shown by a star. B. Schematic cross-section A-A' through the Baltimore area, after Fisher *et al.* (1979). The stippled pattern represents the Baltimore Gneiss; the diagonal line pattern represents the Cocksylville and Setters Formations combined. The unpatterned area is the Loch Raven Formation, and the horizontal line pattern represents the Baltimore Mafic Complex.

component systems may be inadequate for a number of reasons, Greenwood (1967, 1968) proposed that mass-balance relationships could be examined in the full n -component system by algebraic analysis using matrices or regression analysis. Computer techniques for examination of reaction relationships among and within metamorphic assemblages, which culminated in LSQPROTEUS (Pigage 1982), were developed in Greenwood's laboratory. The algebraic approach has, however, seldom been used to analyze metamorphic assemblages (Fletcher & Greenwood 1979, Pigage 1976, 1982, Lang & Rice 1985a, Giaramita & Day 1989), perhaps in part because the techniques are somewhat cumbersome to use. Fisher (1988, 1989) recently proposed that the algebraic technique called Singular Value Decomposition (SVD) could be applied in a straightforward fashion to identify mass-balance relationships within and between metamorphic assemblages. The SVD technique is used here to examine mass-balance relationships between pairs of metamorphic assemblages.

A 0.5-km-long two-tiered roadcut in pelitic schists north of the Hunt Valley Mall in Cockeysville, Maryland (Figs. 1, 2) provides an excellent opportunity to study the relative effects of variation in intensive parameters and variation in bulk composition in staurolite-kyanite-grade metapelites. At this exposure, rocks with abundant staurolite, garnet and biotite (St assemblage) alternate in an unsystematic fashion with rocks with abundant kyanite, minor staurolite, garnet and biotite (St-Ky assemblage). In this study, detailed petrographic analysis, thermobarometry using the GE \emptyset -CALC program TWEEQU (Brown *et al.* 1988, 1989, Berman 1991), graphical analysis and algebraic analysis using SVD (Fisher 1989) are applied to the St and St-Ky assemblages from Hunt Valley Mall in order to determine the conditions that formed them. Particular attention is focused on a determination of the relative roles of variation in bulk composition and in intensive variables (particularly fluid composition) as controls of the difference in the assemblage of metamorphic minerals observed.

GEOLOGICAL SETTING

Rocks that are exposed at Hunt Valley Mall, located approximately 10 km north of the Baltimore Beltway (I-695) east of I-83 on Shawan Road, belong to the Baltimore Gneiss Terrane of the central Appalachian Piedmont (Fig. 1A). The Grenville-age Baltimore Gneiss and overlying sediments were thrust northwestward into a nappe structure and metamorphosed during the Or-

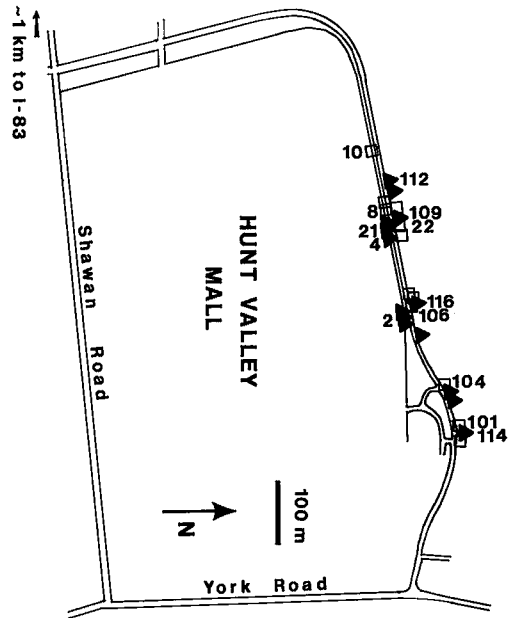


FIG. 2. Metamorphic assemblage and sample location map for the Hunt Valley Mall exposure (latitude $39^{\circ}30'N$, longitude $76^{\circ}39.5'W$). Samples with the St assemblage (garnet, biotite, staurolite, quartz, muscovite, plagioclase, ilmenite \pm magnetite) are indicated by a filled triangle. Samples with the St-Ky assemblage (garnet, biotite, minor staurolite, kyanite, quartz, muscovite, plagioclase, ilmenite \pm rutile \pm pyrrhotite) are indicated by open squares. Sample numbers of analyzed samples are shown alongside the appropriate symbol. Prefixes for all sample numbers are HV except for MD21 and MD22.

dovician Taconic Orogeny (Fig. 1B; Crowley *et al.* 1976, Fisher *et al.* 1979, Muller & Chapin 1984, Sinha 1988). Metasedimentary units exposed in the area surrounding the Baltimore Gneiss include quartzites and pelites of the Setters Formation, the Cockeysville Marble and pelitic schists of the Loch Raven Schist (Fig. 1A). The unit exposed at Hunt Valley Mall is the garnet schist member of the Setters Formation (Crowley *et al.* 1976), which directly overlies the Baltimore Gneiss at that location.

Three stages of deformation approximately synchronous with metamorphism affected pelitic schists in the Baltimore Gneiss Terrane. These stages correspond to the $F2a$, $F2b$ and $F2c$ generations of folding recognized by Muller & Chapin (1984) in the Baltimore Gneiss; these were caused by collision of the Baltimore Complex island-arc terrane with the Baltimore Gneiss Terrane during the Ordovician Taconic Orogeny (Sinha 1988). $F2a$ was attributed to nappe formation by Muller & Chapin (1984). $F2b$, which was

primarily a flattening deformation, refolded the nappe(s) (Fig. 1B), produced the dominant schistosity, and is responsible for the map pattern of gneiss-cored anticlines (Fig. 1A). *F2c* produced mesoscopic folds with horizontal axial planes and crenulated the *F2b* foliation.

MINERAL ASSEMBLAGES AND TEXTURES

Excavation for the Hunt Valley Mall in Cockeysville, 22 km north of Baltimore, Maryland, in 1980 exposed relatively fresh pelitic schist for about 0.5 km along the north side of the parking lot and for a similar distance about 30 m above and to the north along the by-pass road (Fig. 2). Two mineral assemblages are common in samples from these exposures (Fig. 2, Table 1). One contains abundant, commonly porphyroblastic staurolite, garnet, biotite, quartz, muscovite, plagioclase (which commonly occurs as ovoid porphyroblasts), ilmenite (or rutile-ilmenite intergrowths, see below) and magnetite (Fig. 3A, St assemblage). The other pelitic assemblage contains abundant kyanite, only minor, fine-grained staurolite, garnet, biotite, quartz, muscovite, plagioclase, ilmenite, rutile and pyrrhotite (Fig. 3B, St-Ky assemblage). No graphite has been observed in either assemblage.

Some St and some St-Ky assemblages contain small amounts of chlorite (Table 1). Chlorite that occurs commonly as inclusions in the cores of garnet porphyroblasts is not in equilibrium with the matrix assemblage. Some chlorite, which occurs interleaved with biotite or along fractures in garnet, is clearly retrograde. Chlorite that occurs in the matrix of some samples is texturally ambiguous and may be part of the peak metamorphic assemblage. Matrix chlorite in five Hunt Valley Mall samples (two with the St assemblage, three with the St-Ky assemblage; see Table 2) was analyzed. Chlorite in four of the five samples is more Mg-rich than coexisting biotite and yields an average K_D [(Mg/Fe)_{bio}/(Mg/Fe)_{chl}] of 0.89, which is similar to the K_D of chlorite and biotite in equilibrium with staurolite, garnet and kyanite in regional metamorphic rocks from the Snow Peak area in northern Idaho (Lang & Rice 1985b). It is, therefore, concluded that chlorite may have been part of the equilibrium peak metamorphic assemblage in some St and St-Ky samples. Chlorite in some samples (such as HV8) that is more Fe-rich than coexisting biotite is probably retrograde. Chlorite is not included in the thermobarometric analysis, but it has been included in some of the mass-balance calculations.

TABLE 1. MINERAL ASSEMBLAGES IN ANALYZED SAMPLES

SAMPLE NUMBER	Chl	Bt	Grt	St	Ky	Sil	Mag	Ilm	Rt	Po
MD21.1 ¹		X	X	X		m ²	X	X ³	m	
MD22.2	m	X	X	X	X	m		X	X	X
HV2.1		X	X	X		m		X ³		
HV4.2	m	X	X	X		m	X	X ³		
HV8H	m	X	X	X	X	m		X	X	
HV10H		X	X	X	X	m		X	m	X
HV101.1		X	X	X	X	m		X	X	X
HV104.1	m	X	X	X	X	m		X	X	X
HV106.1		X	X	X	X	m		X	X	X
HV109.2		X	X	X		m	?	X ³		m
HV112.2		X	X	X		m	X	X ³		
HV114.2	m	X	X	X		m		X		X ⁴
HV116.2		X	X	X		m	X	X		

¹ All samples contain muscovite, quartz and plagioclase in addition to the minerals indicated in the Table. Samples with numbers in **bold** typeface contain staurolite without kyanite, and are referred to as St assemblages; samples with numbers in regular type contain staurolite and kyanite, and are referred to as St-Ky assemblages.

² m indicates the occurrence of a few fine prisms of late silimanite in the sample (if in the Sil column), minor rutile or sulfide (if in the Rt or Po column), or minor chlorite (if in the Chl column).

³ Sample contains ilmenite-rutile intergrowths. See text for discussion.

⁴ This sample contains a sulfide cluster with pyrrhotite, chalcopyrite, and pyrite.

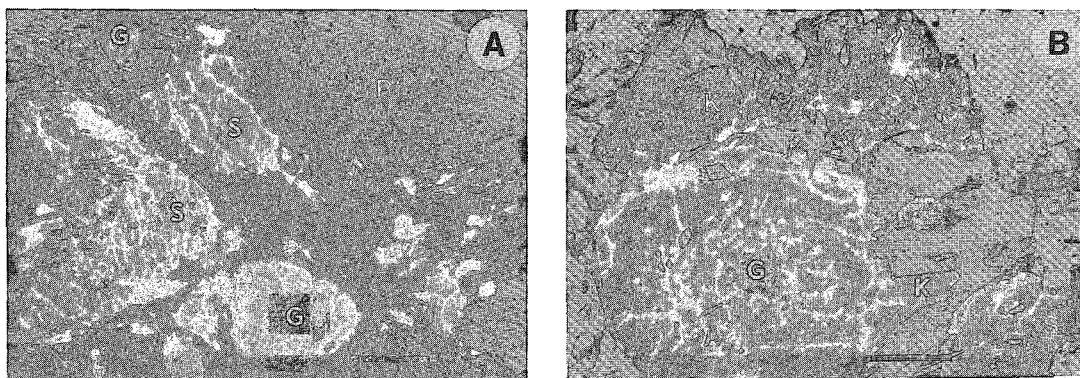


FIG. 3. A. Photomicrograph of a representative St assemblage (MD21.1). Staurolite (S), garnet (G), biotite (dark), and muscovite are abundant. Note the poikiloblastic plagioclase (P) porphyroblast in the upper right corner of the field (plane-polarized light, scale bar 2 mm). B. Photomicrograph of an example of the St-Ky assemblage (HV10H). Garnet (G), staurolite (S), and kyanite (K) are indicated on the photograph (plane-polarized light, scale bar is 0.5 mm).

TABLE 2. SUMMARY OF MINERAL COMPOSITION DATA

	GARNET COMPONENTS				BIOTITE ¹						PLAGIOCLASE		
	X(Alm)	X(Prp)	X(Grs)	X(Sps)	X(Mg)	X(Fe)	X(Ti)	X(^{vi} Al)	X(K)	X(OH)	X(An)	X(Ab)	X(Or)
MD21.1	0.812	0.131	0.022	0.035	0.424	0.396	0.036	0.143	0.943	0.944	0.046	0.951	0.003
MD22.2	0.778	0.139	0.066	0.016	0.425	0.400	0.038	0.136	0.961	0.944	0.251	0.743	0.007
HV2.1	0.782	0.146	0.021	0.051	0.445	0.394	0.031	0.129	0.948	0.935	0.082	0.915	0.003
HV4.2	0.797	0.152	0.012	0.038	0.433	0.383	0.031	0.152	0.944	0.948	0.032	0.965	0.002
HV8H	0.757	0.162	0.064	0.017	0.465	0.359	0.035	0.141	0.957	0.944	0.263	0.733	0.004
HV10H	0.747	0.161	0.070	0.023	0.451	0.360	0.037	0.151	0.948	0.949	0.290	0.707	0.003
HV101.1	0.750	0.164	0.051	0.035	0.462	0.343	0.034	0.160	0.958	0.958	0.229	0.767	0.004
HV104.1	0.778	0.156	0.050	0.016	0.447	0.381	0.031	0.140	0.961	0.954	0.225	0.771	0.003
HV106.1	0.751	0.165	0.045	0.039	0.460	0.362	0.035	0.142	0.946	0.948	0.195	0.802	0.003
HV109.2	0.772	0.146	0.029	0.053	0.463	0.370	0.029	0.136	0.932	0.952	0.233	0.763	0.004
HV112.2	0.730	0.166	0.018	0.086	0.503	0.327	0.031	0.136	0.940	0.943	0.084	0.914	0.002
HV114.2	0.778	0.146	0.041	0.035	0.425	0.404	0.035	0.135	0.961	0.959	0.168	0.829	0.003
HV116.2	0.778	0.141	0.034	0.048	0.434	0.393	0.029	0.142	0.938	0.952	0.143	0.855	0.002
	MUSCOVITE ²				STAUROLITE ³			"ILMENITE" ⁴		CHLORITE ⁵			
	X(K)	X(Na)	X(^{vi} Al)	X(OH)	X(Fe)	X(Mg)	X(Zn)	Fe	Ti	X(Mg)			
MD21.1	0.767	0.233	0.871	0.989	0.802	0.183	0.008	0.621	1.172				
MD22.2	0.838	0.162	0.897	0.989	0.766	0.189	0.042	1.020	0.971	0.539			
HV2.1	0.761	0.236	0.879	0.991	0.791	0.188	0.014	0.834	1.029				
HV4.2	0.757	0.240	0.888	0.989	0.788	0.194	0.012	0.759	1.078	0.572			
HV8H	0.821	0.177	0.888	0.998	0.766	0.199	0.032	0.966	0.966	0.550			
HV10H	0.841	0.156	0.892	0.994	0.733	0.206	0.057	0.969	0.994				
HV101.1	0.829	0.167	0.905	0.996	0.729	0.198	0.066	0.980	0.983	0.543			
HV104.1	0.827	0.169	0.906	0.994	0.730	0.193	0.074	0.974	0.988				
HV106.1	0.823	0.174	0.904	0.995	0.726	0.201	0.080	0.958	0.996				
HV109.2	0.807	0.188	0.877	0.994	0.780	0.202	0.007						
HV112.2	0.771	0.228	0.878	0.994	0.758	0.220	0.008	0.719	1.106				
HV114.2	0.788	0.211	0.871	0.991	0.788	0.191	0.016	1.061	0.951	0.547			
HV116.2	0.773	0.223	0.890	0.994	0.799	0.190	0.005	1.103	0.931				

¹ Biotite: X(Mg) = Mg/(Mg+Fe+Mn+Ti+^{vi}Al), X(Fe) = Fe/(Mg+Fe+Mn+Ti+^{vi}Al), X(Ti) = Ti/(Mg+Fe+Mn+Ti+^{vi}Al), X(^{vi}Al) = ^{vi}Al/(Mg+Fe+Mn+Ti+^{vi}Al), X(K) = K/(K+Na), X(OH) = OH/(OH+F)

² Muscovite: X(K) = K/(K+Na+Ca), X(Na) = Na/(K+Na+Ca), X(^{vi}Al) = ^{vi}Al/(Mg+Fe+Ti+^{vi}Al), X(OH) = OH/(OH+F)

³ Staurolite: X(Fe) = Fe/(Fe+Mg+Mn+Zn), X(Mg) = Mg/(Fe+Mg+Mn+Zn), X(Zn) = Zn/(Fe+Mg+Mn+Zn)

⁴ "Ilmenite" (ilmenite or ilmenite-rutile intergrowth): Fe = cations Fe (as Fe²⁺) per 3 oxygen atoms, Ti = cations Ti per 3 oxygen atoms

⁵ Chlorite: X(Mg) = Mg/(Mg+Fe+Mn)

The distribution of samples with the St assemblage (filled triangles in Fig. 2) and samples with the St-Ky assemblage (open squares) is not

systematic along the exposure. Samples with the St assemblage and samples with the St-Ky assemblage were collected very close to one another. The small

size of the exposure, the lack of systematic distribution of the two assemblages, and the close proximity of St and St-Ky assemblages have led to the inference that variation in temperature and total pressure cannot explain the variation in metamorphic mineral assemblage of these pelitic rocks.

St and St-Ky samples have distinct textures as well as assemblages. Textures in St-Ky samples indicate that garnet growth began after *F2a* and probably continued at least through *F2b*, staurolite grew during *F2b*, and kyanite growth was mainly post-*F2b* and pre-*F2c* (Hall 1988). Garnet in St-Ky samples ranges from 3 to 7 mm in diameter. Garnet cores contain fine planar trails of inclusions that are generally at a high angle to the external foliation. This texture is interpreted to indicate that garnet cores grew subsequent to formation of *S2a* foliation, but prior to transposition of that foliation by development of crenulation cleavage into *S2b*, the dominant foliation (Hall 1988). Garnet rims, which are relatively inclusion-free, may have continued to grow during *F2b* folding. Staurolite in St-Ky samples occurs as small poikiloblasts that commonly contain sigmoidal trails of medium-sized quartz inclusions, which indicate that staurolite grew mainly during *F2b* deformation (Bell & Rubenach 1983). Kyanite porphyroblasts grew over the *F2b* mica foliation, commonly mimicking it. Kyanite grains contain few inclusions; they may have begun to grow during *F2b*, but are mainly postkinematic to *F2b*. Kyanite and, by implication, garnet and staurolite, were clearly pre-*F2c* in St-Ky samples, because the kyanite has been bent and kinked by minor *F2c* folding. Matrix muscovite and biotite define the dominant foliation (*S2b*); however, that foliation was subsequently crenulated by *F2c*. The common occurrence of muscovite that cross-cuts the *S2b* foliation indicates considerable post-*F2b* recrystallization of muscovite.

Textures of St samples indicate sequential growth of garnet, staurolite and plagioclase porphyroblasts, but, in some St samples, most crystallization or recrystallization of porphyroblasts seems to have occurred *after* deformation. These St samples contain small grains of inclusion-free garnet 1–2 mm in diameter. In some St assemblages, garnet clearly grew over the *F2b* muscovite foliation (Hall 1988). Staurolite occurs as randomly oriented, hypidioblastic porphyroblasts (0.5 to 2.0 cm in diameter) that contain relatively rare trails of quartz and ilmenite inclusions, which are generally parallel to the external foliation. Staurolite porphyroblasts commonly contain grains of garnet that are nearly identical in size and appearance to those external to the staurolite. Some staurolite and garnet are included in ovoid plagioclase porphyroblasts up to

3 cm in diameter (Fig. 3A). These plagioclase porphyroblasts appear to have grown subsequent to all major deformation, as they contain trails of inclusions that show *F2c* crenulations of the *F2b* foliation and lack deformation twins (Fig. 4A). Some St-Ky assemblages also contain plagioclase porphyroblasts, which also are postkinematic.

Plagioclase porphyroblasts are nearly pure albite in most, but not all, St samples and, although it is difficult to estimate modes, they comprise as much as 20% of some portions of the outcrop. The abundance of sodic plagioclase in some St samples suggests that those samples have an unusually Na-rich bulk composition. The sodium-rich bulk composition may have been a feature of the sedimentary protolith, or sodium may have been introduced by a metasomatic fluid during metamorphism. A peculiar texture that has been observed in a few samples with plagioclase porphyroblasts (Figs. 4B, C) suggests that metasomatic introduction of sodium and removal or redistribution of potassium and iron may account for the abundance of sodic plagioclase in these samples. Some staurolite included in plagioclase porphyroblasts appears to have been partially consumed by the engulfing plagioclase (Figs. 4B, C). Fingers and blebs of optically continuous staurolite are surrounded by twinned plagioclase, and quartz "islands," which appear to have originated as inclusions in staurolite, remain in the plagioclase (Figs. 4B, C). Garnet is apparently unaffected by being incorporated into plagioclase porphyroblasts. Muscovite in the matrix of most samples is coarse grained and strongly oriented, although there is some randomly oriented muscovite as a result of post-*F2b* crenulation and recrystallization. Within the plagioclase porphyroblasts, inclusions of much finer muscovite define sets of planar trails with some crenulations (Figs. 4A, C). The very planar nature of the trails of muscovite inclusions suggests that there is some crystallographic control on which muscovite grains are retained as inclusions. Again, replacement of the muscovite-rich matrix by plagioclase suggests metasomatic introduction of sodium and removal of potassium.

There is no textural evidence that kyanite was ever present in the St samples. Most St samples contain magnetite and ilmenite or rutile-ilmenite intergrowths (Table 1). Although the outcrop was exposed only recently and the samples appear to be relatively fresh, the fine-grained intergrowths of rutile with hematite or ilmenite may be a product of supergene alteration of ferrian ilmenite (Rumble 1976, pers. comm., 1990). No graphite or sulfide was observed in St samples.

All samples from the Hunt Valley Mall exposure, both St and St-Ky assemblages, contain very small

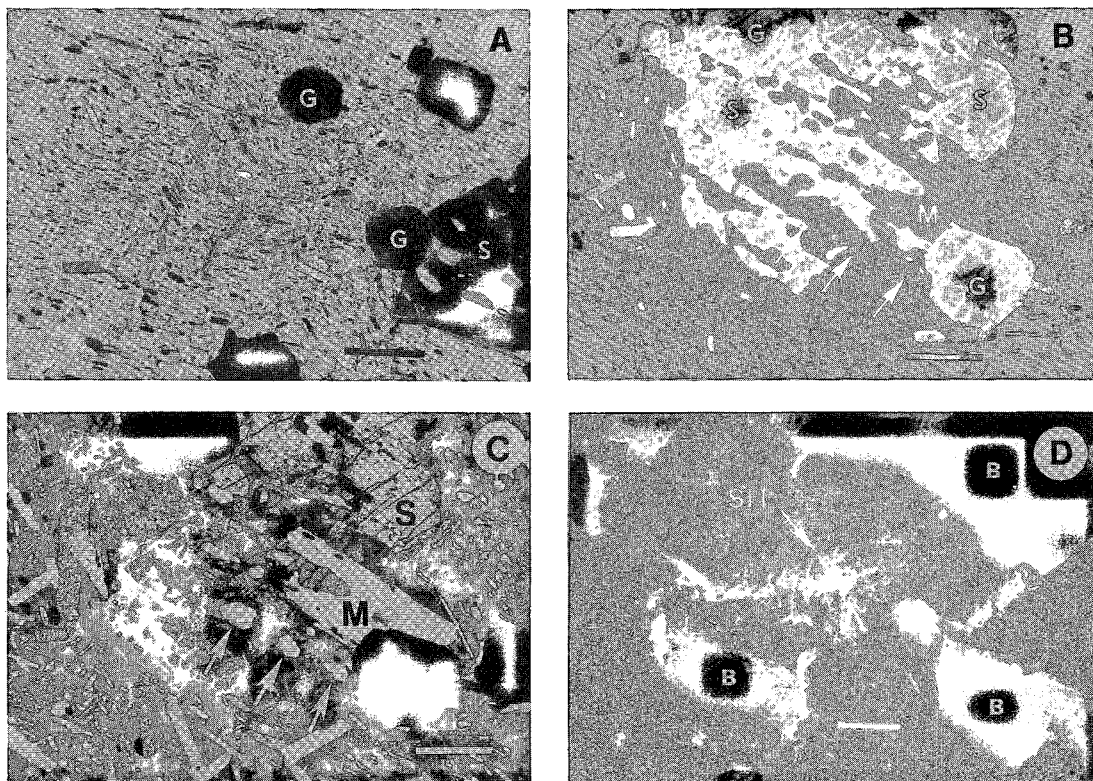


FIG. 4. A. Photomicrograph of a plagioclase porphyroblast (entire bright field is plagioclase) with crenulated trails of inclusions (upper left to lower right) composed of muscovite, ilmenite and quartz. Garnet (G) and staurolite (S) inclusions are indicated (crossed-polarized light, scale bar is 2 mm, sample HV7.1). B. Photomicrograph of a staurolite porphyroblast (S, all the high-relief material except garnet G), which appears to have been partly consumed by the plagioclase porphyroblast that surrounds it (see also 4C; HV7.1, plane-polarized light, scale bar is 0.5 mm, M muscovite); arrows point to quartz inclusions in plagioclase that appear to have been inherited from replaced staurolite. C. Same field as 4B in crossed-polarized light. Note albite twinning and inclusion trails in surrounding plagioclase (P, upper right and along base of photograph). Arrows point to quartz inclusions inherited from staurolite. Scale bar is 0.5 mm. D. Photomicrograph of fine-grained, randomly oriented, postkinematic sillimanite that occurs in small amounts in most Hunt Valley Mall samples. HV8V; plane-polarized light; dark grains are biotite, colorless matrix is mostly plagioclase; scale bar is 0.1 mm.

amounts of fine, postkinematic sillimanite (Fig. 4D). This sillimanite probably formed during decompression; its significance will be discussed below.

ELECTRON-MICROPROBE DATA

Mineral compositions were determined by analyzing carbon-coated, polished thin sections on the ARL-SEMQ microprobe at Virginia Polytechnic Institute and State University. Operating conditions were: accelerating potential 15 kv, and beam current 20 nA. A focused beam $\sim 1 \mu\text{m}$ in diameter was used for garnet and other minerals in which volatile loss was not likely to be a problem. A $4 \times 4 \mu\text{m}$ raster was used for the micas and

plagioclase to avoid loss of volatile elements. Standard nine-element analyses were done for most minerals. Eighteen-element analyses (Solberg & Speer 1982) were done on a few grains of staurolite, biotite, and muscovite in each sample in order to determine concentrations of Zn and F, and to detect other minor elements. Well-characterized natural standards were used for most elements; synthetic oxide or glass standards were used for a few minor elements. Data reduction was performed according to the procedure of Bence & Albee (1968) with the alpha factors of Albee & Ray (1970). All iron is reported as FeO.

Quartz, kyanite, and sillimanite were assumed to be pure. The other major minerals (biotite, garnet, staurolite, plagioclase, muscovite, ilmenite, mag-

netite, and sulfide) in samples from the twelve localities shown in Figure 2 were analyzed. Garnet in Hunt Valley samples is weakly to strongly zoned. Although zoning patterns are complex, grossular and spessartine contents generally decrease, and almandine and pyrope contents increase, from core to rim of individual grains of garnet (Lang, unpubl. data). Plagioclase in some samples is zoned, although the zoning is not systematic and has not been thoroughly investigated. Five to six spots on rims of each mineral in each sample were analyzed. Rim compositions are reported and used in the calculations. A summary of data on mineral compositions is given in Table 2. A sense of the amount of variation in mineral compositions can be obtained from the error files for SVD analysis (*ERR in Tables 5 & 6), which contain the standard deviation of the several analyses of each element in each mineral.

Analyses ($4 \times 4 \mu\text{m}$ raster) of "ilmenite" in four St samples (HV2.1, HV4.2, HV112.2, and MD21.1) yielded Ti-excess Fe-Ti oxides. Further examination (Fig. 5) of such "ilmenite" grains shows that they are composed of fine-grained intergrowths of rutile, ilmenite, hematite and corundum (Table 3). A back-scattered electron image of one of the grains with rutile-ilmenite intergrowths (HV2.1) is shown in Figure 5. Semiquantitative energy-dispersion analyses of several spots (Table 3) show the range of variation in composition of these grains. Rumble (1976, pers. comm., 1990) suggested that such intergrowths result from supergene alteration of ferrian ilmenite. The rutile-ilmenite intergrowths are absent from St-Ky samples, perhaps because these contain more nearly pure ilmenite rather than

TABLE 3. SEMIQUANTITATIVE DETERMINATION OF COMPOSITION OF "RUTILE-ILMENITE" INTERGROWTHS IN ST SAMPLE HV2.1

Location (see Fig. 5)	A	B	D	E	1	2
Al	0.0	0.0	0.0	53.6	1.0	16.6
Si	0.0	0.0	0.0	2.0	59.0	1.5
Ti	45.7	46.3	97.3	21.4	28.4	57.3
Fe	54.3	53.6	2.2	23.1	11.5	24.6

Location	3	4	5	7	8	13
Al	0.0	0.0	27.5	0.0	0.0	0.0
Si	0.0	0.0	1.7	0.0	0.0	0.0
Ti	81.0	87.1	48.1	11.0	22.2	73.3
Fe	18.6	12.9	22.7	89.0	77.4	26.7

* by energy-dispersion analysis, SEM. Results are quoted in atomic percent.

ferrian ilmenite, which is more susceptible to supergene alteration (Rumble 1976).

THERMOBAROMETRY

Although there is textural evidence that porphyroblasts in some of the St samples crystallized or recrystallized later in the deformation sequence than those in the St-Ky samples, the close proximity and random distribution of the two assemblages on the outcrop scale, the lack of retrograde effects in St-Ky samples and the presence of late sillimanite in both assemblages indicate that both assemblages last equilibrated at the same temperature (T) and total pressure (P). An estimate of the temperature and total pressure

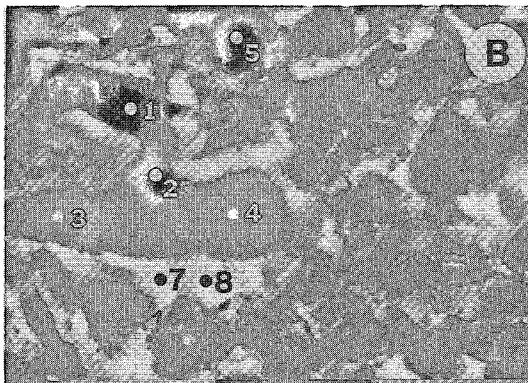
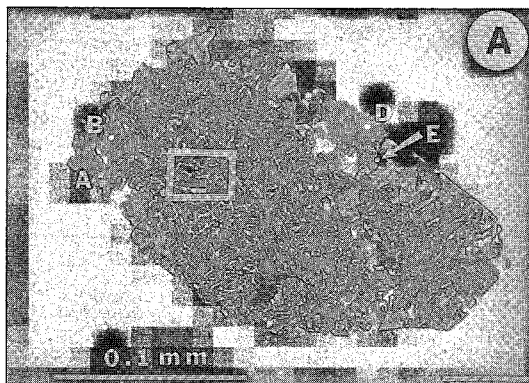


FIG. 5. A. Low-magnification SEM back-scattered electron image of an oxide grain from HV2.1 that shows the rutile-ilmenite-hematite intergrowths that are common in St samples. Results of analyses of points A, B, D and E are given in Table 3. The white rectangle shows the location of the image of Fig. 5B. B. Higher-magnification SEM back-scattered electron image of a portion of the grain shown in Fig. 5A. Analyses taken at points 1, 2, 3, 4, 5, 7, 8 and 13 are given in Table 3. Alternating light and dark scale bars at the base of the photograph are each $10 \mu\text{m}$ in length.

to which these rocks were exposed during metamorphism has been made using GE \emptyset -CALC software (Brown *et al.* 1988, 1989), and specifically the TWEEQU program and database (Berman 1988, 1991). The St-Ky assemblage contains mineral components that participate in a large number of pressure- and temperature-sensitive solid-solid equilibria. Figure 6 shows the positions in P-T space of all the solid-solid equilibria among the components of garnet (rim), biotite, muscovite, plagioclase, ilmenite, kyanite, quartz and rutile for two different St-Ky samples (MD22, HV104) from the Hunt Valley Mall exposure. Equilibria were adjusted for mineral compositions using the activity models of Berman (1990) for garnet, McMullin & Berman (1990, 1991) for biotite, Fuhrman & Lindsley (1988) for plagioclase, and Chatterjee & Froese (1975) for muscovite. Staurolite was not included because of uncertainties concerning thermodynamic data. Al₂SiO₅ relationships calculated

with the TWEEQU database (Berman 1991), which relies on Holdaway's (1971) determination of the Al₂SiO₅ diagram, are shown for reference.

MD22 (Fig. 6A) yields a very tight cluster of intersections on the GE \emptyset -CALC P-T diagram. (Note that only four of the equilibria in Fig. 6A are independent.) Other samples yield results more like those for HV104 (Fig. 6B), which give a cluster of high-angle intersections in the vicinity of 6.0 kilobars and 600°C, but have some intersections that are scattered over a range of P and T. Weighted averages of all intersections have been calculated for each St-Ky sample using the GE \emptyset -CALC program TBAV (Table 4; Berman 1991). Average deviations reflecting the amount of scatter in intersections are 20 to 43°C and 0.6 to 1.2 kbar for all samples except HV101, which has a slightly larger uncertainty of $\pm 59^\circ\text{C}$ and ± 1.8 kbar (Table 4). This magnitude of scatter is to be expected in thermobarometry (Hodges & McKenna

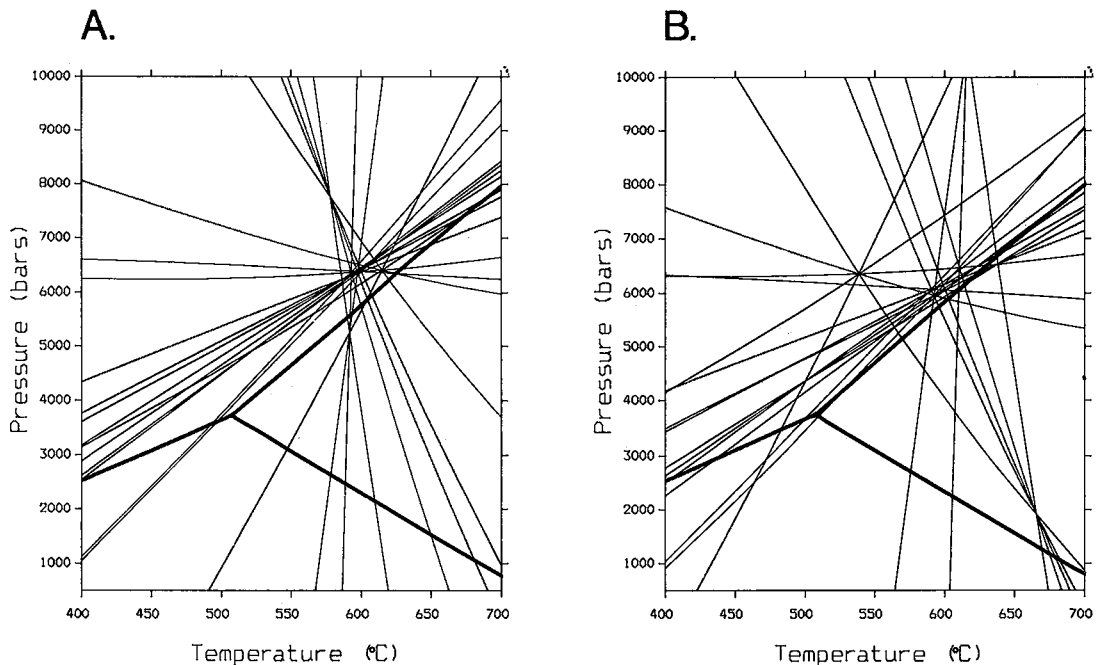


FIG. 6. A. GE \emptyset -CALC (Brown *et al.* 1988, 1989) P-T diagram including all solid-solid equilibria (stable and metastable) among the components of garnet, biotite, muscovite, plagioclase, ilmenite, kyanite, quartz and rutile in the system K₂O-CaO-FeO-MgO-SiO₂-Al₂O₃-TiO₂ adjusted for mineral compositions in St-Ky sample MD22.2 (there are 4 independent reactions). Al₂SiO₅ phase boundaries [from GE \emptyset -CALC, based on Holdaway (1971)] are shown as heavy lines for reference. Activity models used in the calculation (Berman 1990 for garnet, McMullin & Berman 1990, 1991 for biotite, Fuhrman & Lindsley 1988 for plagioclase, and Chatterjee & Froese 1975 for muscovite) are discussed in the text. Labels have been omitted for clarity. Note the tight clustering of intersections in the vicinity of 600°C and 6500 bars. B. A similar GE \emptyset -CALC P-T diagram for St-Ky sample HV104 (4 independent reactions). The clustering of intersections for this and all other St-Ky assemblages is not as tight as for MD22.2; however, most equilibria intersect in a small region near 600°C and 6000 bars. Al₂SiO₅ relations are shown by heavy lines.

TABLE 4. TEMPERATURE AND PRESSURE ESTIMATES
BASED ON GEOCALC

SAMPLE NUMBER	T(avg) (°C)	T(error) (°C)	P(avg) (kbar)	P(error) (kbar)
St-Ky samples (with Ky and Ms)				
MD22	603	±23	6.5	±0.6
HV8	593	±32	6.2	±1.0
HV10	590	±41	6.1	±1.1
HV101	569	±59	5.6	±1.8
HV104	605	±20	6.2	±0.5
HV106	584	±43	6.2	±1.2
Average (St-Ky)	591	±36	6.1	±1.0
St samples (+Sil, +Rt)				
HV114	610	±73	6.9	±1.4
HV116	590	±68	6.6	±1.3

1987, R.G. Berman, pers. comm.). Reactions that involve muscovite seem to show more scatter than those that involve only garnet rims, biotite, plagioclase, ilmenite, kyanite, quartz and rutile, which suggests that there may be problems with the thermodynamic data or activity - composition relationships for muscovite, or that muscovite may have re-equilibrated after the peak of metamorphism. Exclusion analysis with TBAV (Berman 1991) shows, however, that results are improved no further by elimination of muscovite than they are by elimination of kyanite or rutile and ilmenite (R.G. Berman, pers. comm.). Replacement of kyanite by sillimanite (present in small amounts in most samples) in the GEØ-CALC calculations yields similar results (at a temperature and pressure in the kyanite field) for any given St-Ky sample.

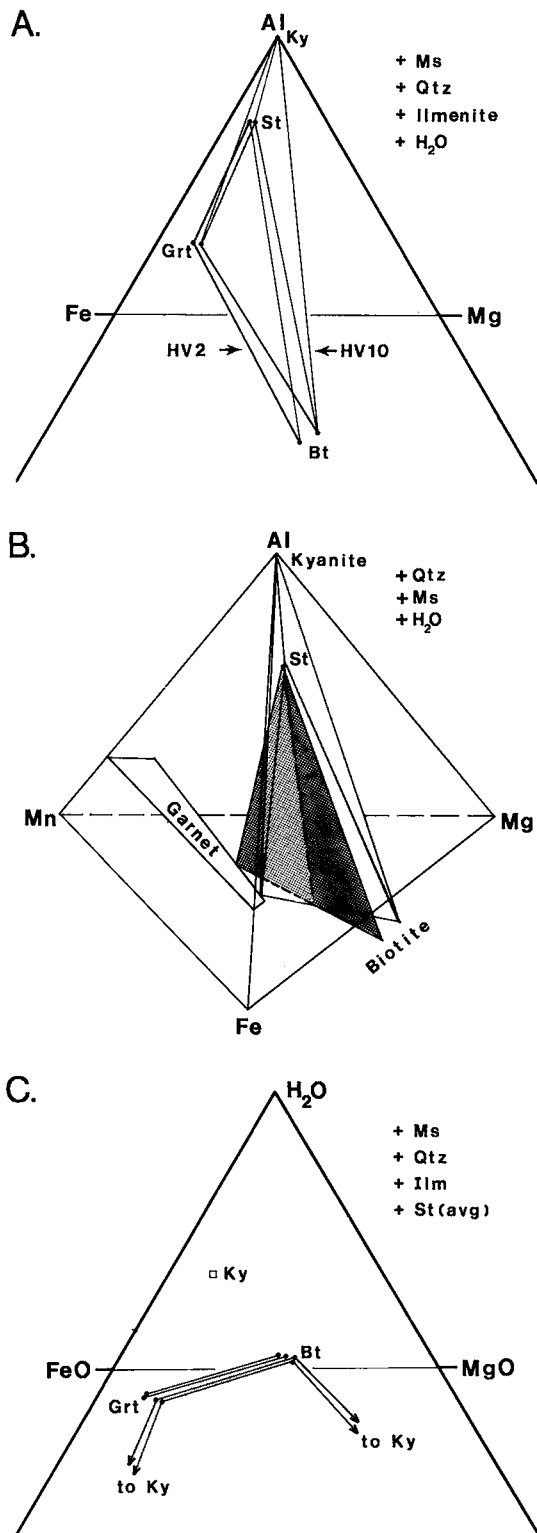
The best estimate of peak metamorphic pressure and temperature conditions for the Hunt Valley Mall exposure is provided by the mean of the TBAV weighted averages for the six St-Ky samples (Table 4), which is 591°C at 6.1 kbar.

The St assemblages contain mineral components of fewer P- and T-sensitive equilibria, and only a single intersection among solid-solid equilibria involving components of garnet (rim), biotite, muscovite, plagioclase, ilmenite and quartz (without staurolite) occurs. The temperature and especially the pressure of this intersection, which does involve muscovite, are somewhat variable, but for some samples, they are near the average value for St-Ky samples. GEØ-CALC P-T diagrams were also calculated for St assemblage minerals plus sillimanite and rutile. Inclusion of sillimanite and rutile in the diagrams is justified by the fact that small amounts of sillimanite are present in all St assemblages, that minor rutile or rutile-ilmenite intergrowths occur in some St samples, and that

the St assemblages may not have been far out of equilibrium with sillimanite or rutile. The clustering of intersections (including sillimanite, muscovite and rutile) is approximately as good for St assemblages (Table 4, HV114 and HV116) as for St-Ky assemblages (with kyanite, muscovite and rutile), except that equilibria involving the anorthite component in plagioclase intersect at a significantly higher or lower pressure than other equilibria in some samples. Because the original composition of ilmenite is unknown in samples with rutile-ilmenite intergrowths, equilibria that involve ilmenite cannot be reliably calculated. Inconsistencies involving anorthite equilibria are most easily accounted for by errors in analyses or in the activity coefficient for anorthite in extremely sodic plagioclase (Table 2). Similar problems have been noted by Berman (1990, 1991) for samples with albite-rich plagioclase. These results suggest that the activities of Al_2SiO_5 and TiO_2 in the St assemblages were very close to unity (Ghent & Gordon 1990). The values of pressure and temperature estimated from the cluster of intersections for St samples are similar to those estimated for St-Ky samples; however, estimates based on St samples are less reliable than those based on St-Ky samples, because the actual activities of Al_2SiO_5 and TiO_2 are unknown. For reasons already stated, adjacent St and St-Ky assemblages must have equilibrated at the same P and T, and the best estimates are 591°C and 6.1 kbar based on equilibria in St-Ky samples.

PROJECTIONS

If temperature and total pressure were nearly constant for rocks from this exposure, the difference in metamorphic assemblage must reflect variation in fluid composition or bulk composition (or both). The relationship between the two assemblages can be examined on appropriate projections. On the AFM diagram (Fig. 7A; Thompson 1957), representative St and St-Ky assemblages exhibit substantial overlap. Other investigators (*e.g.*, Ghent 1975, Lang & Rice 1985a, Spear 1988, Spear & Cheney 1989) have attributed this type of overlap to variation in extra components such as CaO or MnO. The schematic AFM-Mn projection (Fig. 7B) shows that including MnO in the projection does not eliminate intersection of St and St-Ky phase volumes. St assemblages generally contain more Fe-rich biotite and more Mn-rich garnet than the St-Ky assemblages, so that the phase volumes of the two assemblages would cross in AFM-Mn space. In AFM-Ca space, the phase volumes would not generally cross because the St assemblage contains more Fe-rich biotite and more Ca-poor garnet (which commonly coexists



with very sodic plagioclase) than the St-Ky assemblage.

Rumble (1978) and Spear *et al.* (1982) suggested that mineral assemblages in metapelites could be projected from kyanite or staurolite onto FeO-MgO-H₂O in order to show variations in $\mu(\text{H}_2\text{O})$ among assemblages. All of the St and St-Ky assemblages from the Hunt Valley Mall exposure contain staurolite of a very similar composition, and Figure 7C shows a projection of these assemblages from quartz, muscovite, ilmenite and average staurolite onto FeO-MgO-H₂O. Kyanite projects negatively onto the diagram, so that tie-lines to kyanite extend away from the point representing kyanite. Although all of the projected points for garnet and biotite plot very close together and there are some minor inconsistencies, the projection is generally consistent with equilibration of St assemblages at higher values of $\mu(\text{H}_2\text{O})$ than St-Ky assemblages.

Although the FeO-MgO-H₂O projection suggests that the St and St-Ky assemblages equilibrated at different values of $\mu(\text{H}_2\text{O})$, some ambiguities always remain when simplified projections of complex systems are employed. In order to construct this projection, some minor components (*e.g.*, Zn, F, Mn) were ignored, and all assemblages were projected from the same average staurolite and muscovite. Projections such as this one cannot account for uncertainties in mineral analyses. The algebraic approach, which is discussed in the following section, removes some of the ambiguity because it does not require elimination of minor components or projection from average mineral compositions, and it does account for analytical uncertainty.

FIG. 7. A. AFM diagram (Thompson 1957) showing that on this projection St assemblages (*e.g.*, HV2; farthest left triangle connecting Grt, St and Bt) and St-Ky assemblages (*e.g.*, HV10; right-hand triangle connecting Grt, Ky and Bt with St in the interior) overlap significantly. B. Schematic AFM-Mn projection (after Spear 1988) of a St assemblage (shaded) and a St-Ky assemblage (unshaded) showing that, because St assemblages generally contain more Fe-rich biotite and more Mn-rich garnet than St-Ky assemblages, their phase volumes would be expected to intersect. C. H₂O-FeO-MgO projection (after Rumble 1978, Spear *et al.* 1982) of representative St (Grt-Bt) and St-Ky (Grt-Bt to Ky) assemblages. All minerals are projected from quartz, muscovite, ilmenite and average staurolite, which are common to all assemblages. Tie-lines to kyanite extend away from the point representing kyanite, because it projects negatively onto the diagram. Although all points plot very close together, the results are consistent with the suggestion that St assemblages equilibrated at higher $\mu(\text{H}_2\text{O})$ than St-Ky assemblages.

ALGEBRAIC ANALYSIS

The algebraic technique of Singular Value Decomposition (SVD; Fisher 1988, 1989) was applied in an attempt to quantify the reaction relationship between St assemblages and St-Ky assemblages that is suggested by the AFM-Mn projection. To examine the relationship between two assemblages by SVD, one forms the composite matrix that contains the phases of Assemblage 1 on the left in terms of convenient components (moles of cations), and the phases of Assemblage 2 alongside them on the right (Tables 5 and 6; Fisher 1989). The SVD programs, which were kindly provided by G.W. Fisher, determine the

rank of the composite matrix and an orthonormal basis for the reaction space from which all possible reaction-relationships between minerals of the two assemblages can be calculated. The models were weighted by the inverse of the standard deviation among individual analyses for each element in each mineral; however, unweighted models gave identical results. The program MULTI (Fisher 1989) calculates all possible reactions and examines them for incompatibilities between the two assemblages, *i.e.*, those reactions for which minerals from one assemblage are reactants, and minerals from the other are products. SVD is more easily applied to pairs of mineral assemblages than LSQPROTEUS (Greenwood 1967, 1968, Pigage 1982, Fisher 1989)

TABLE 5. SVD DATA AND ERROR FILES FOR SAMPLES HV2 (St ASSEMBLAGE) AND HV106 (St-Ky ASSEMBLAGE)

HV2-HV106.DAT (cations/formula unit)														
	Grt2	Bt2	Ilm12	St2	Ms2	Pl2	Ky	Grt106	Bt106	Ilm106	St106	Ms106	Pl106	Rt
Si	2.955	5.318	0.013	7.839	6.055	2.839	1.000	3.000	5.403	0.003	7.961	6.139	2.765	0.000
Ti	0.007	0.182	1.029	0.138	0.063	0.001	0.000	0.006	0.205	0.996	0.163	0.086	0.001	1.000
Al	1.984	3.435	0.038	17.691	5.575	1.176	2.000	1.997	3.420	0.004	17.569	5.568	1.251	0.000
Fe	2.423	2.307	0.834	3.316	0.256	0.003	0.000	2.244	2.099	0.958	3.021	0.120	0.004	0.000
Mn	0.157	0.009	0.007	0.030	0.001	0.000	0.000	0.118	0.007	0.012	0.027	0.001	0.001	0.000
Mg	0.452	2.608	0.010	0.789	0.179	0.011	0.000	0.493	2.669	0.022	0.852	0.188	0.012	0.000
Ca	0.055	0.010	0.004	0.008	0.006	0.082	0.000	0.135	0.010	0.002	0.008	0.004	0.188	0.000
Na	0.001	0.092	0.002	0.014	0.452	0.918	0.000	0.003	0.090	0.000	0.036	0.308	0.772	0.000
K	0.004	1.685	0.002	0.008	1.460	0.003	0.000	0.003	1.591	0.002	0.006	1.455	0.003	0.000
F	0.000	0.259	0.000	0.000	0.034	0.000	0.000	0.000	0.209	0.000	0.000	0.019	0.000	0.000

HV2-HV106.ERR (standard deviations)														
	sdgrt2 n=6	sdbt2 n=5	sdrt112 n=5	sdst2 n=6	sdms2 n=8	sdpl2 n=6	sdky n=1	sdgrt106 n=5	sdbt106 n=7	sdilm106 n=3	sdst106 n=3	sdms106 n=7	sdpl106 n=5	sdrt n=1
Si	0.028	0.055	0.003	0.115	0.065	0.017	0.002	0.034	0.012	0.001	0.083	0.028	0.006	0.002
Ti	0.001	0.009	0.055	0.011	0.005	0.002	0.002	0.002	0.031	0.001	0.010	0.006	0.002	0.002
Al	0.046	0.131	0.025	0.115	0.096	0.024	0.002	0.033	0.033	0.002	0.083	0.045	0.009	0.002
Fe	0.030	0.034	0.097	0.114	0.016	0.002	0.002	0.022	0.034	0.005	0.020	0.003	0.001	0.002
Mn	0.004	0.003	0.010	0.005	0.002	0.002	0.002	0.014	0.001	0.001	0.004	0.001	0.002	0.002
Mg	0.018	0.058	0.002	0.021	0.019	0.001	0.002	0.019	0.047	0.002	0.010	0.013	0.001	0.002
Ca	0.003	0.003	0.002	0.002	0.003	0.006	0.002	0.008	0.007	0.002	0.001	0.001	0.004	0.002
Na	0.002	0.008	0.001	0.011	0.025	0.009	0.002	0.001	0.008	0.001	0.010	0.025	0.010	0.002
K	0.001	0.025	0.002	0.002	0.028	0.002	0.002	0.001	0.036	0.002	0.001	0.041	0.001	0.002
F	0.002	0.002	0.002	0.002	0.002	0.002	0.002	0.002	0.009	0.002	0.002	0.008	0.002	0.002

TABLE 6. SVD DATA AND ERROR FILES FOR SAMPLES HV114 (St ASSEMBLAGE) AND HV101 (St-Ky ASSEMBLAGE)

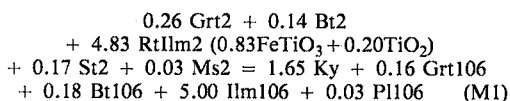
HV114-HV101.DAT (cations/formula unit)															
	Chl114	Grt114	Bt114	Ilm114	St114	Ms114	Pl114	Ky	Grt101	Bt101	Ilm101	St101	Ms101	Pl101	Rt
Si	2.609	3.001	5.393	0.003	7.870	6.150	2.786	1.000	2.999	5.375	0.002	7.847	6.182	2.725	0.000
Ti	0.012	0.007	0.203	0.951	0.134	0.068	0.001	0.000	0.006	0.199	0.983	0.142	0.081	0.001	1.000
Al	2.805	2.000	3.389	0.002	17.660	5.440	1.228	2.000	2.002	3.552	0.009	17.683	5.510	1.283	0.000
Fe	2.043	2.319	2.345	1.061	3.298	0.280	0.005	0.000	2.238	1.983	0.980	2.906	0.122	0.002	0.000
Mn	0.007	0.103	0.007	0.007	0.020	0.001	0.000	0.000	0.106	0.007	0.020	0.029	0.001	0.000	0.000
Mg	2.494	0.436	2.463	0.016	0.799	0.185	0.012	0.000	0.489	2.671	0.012	0.788	0.187	0.012	0.000
Ca	0.003	0.123	0.010	0.003	0.003	0.003	0.163	0.000	0.151	0.013	0.003	0.009	0.007	0.227	0.000
Na	0.002	0.003	0.068	0.002	0.007	0.392	0.805	0.000	0.002	0.069	0.001	0.033	0.300	0.761	0.000
K	0.007	0.004	1.678	0.003	0.003	1.465	0.002	0.000	0.004	1.599	0.003	0.005	1.485	0.004	0.000

HV114-101.ERR (standard deviations)															
	sdchl114 n=5	sdgrt114 n=6	sdbt114 n=6	sdilm114 n=1	sdst114 n=6	sdms114 n=6	sdpl114 n=6	sdky n=1	sdgrt101 n=6	sdbt101 n=6	sdilm101 n=3	sdst101 n=7	sdms101 n=6	sdpl101 n=6	sdrt n=1
Si	0.026	0.035	0.047	0.002	0.096	0.037	0.026	0.002	0.022	0.063	0.001	0.075	0.051	0.025	0.002
Ti	0.001	0.001	0.018	0.002	0.010	0.006	0.002	0.002	0.001	0.029	0.008	0.033	0.005	0.002	0.002
Al	0.095	0.044	0.065	0.002	0.096	0.036	0.039	0.002	0.019	0.184	0.010	0.075	0.075	0.034	0.002
Fe	0.047	0.010	0.104	0.002	0.041	0.012	0.003	0.002	0.033	0.133	0.029	0.088	0.005	0.001	0.002
Mn	0.004	0.001	0.001	0.002	0.003	0.001	0.002	0.002	0.007	0.001	0.002	0.008	0.001	0.002	0.002
Mg	0.113	0.021	0.059	0.002	0.044	0.008	0.001	0.002	0.028	0.098	0.002	0.058	0.014	0.002	0.002
Ca	0.002	0.007	0.004	0.002	0.003	0.002	0.014	0.002	0.022	0.005	0.002	0.004	0.002	0.004	0.002
Na	0.002	0.003	0.011	0.002	0.007	0.027	0.020	0.002	0.002	0.008	0.001	0.012	0.025	0.008	0.002
K	0.007	0.001	0.044	0.002	0.002	0.014	0.002	0.002	0.001	0.058	0.001	0.002	0.045	0.002	0.002

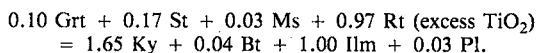
because it can handle systems in which there are more minerals than components. SiO_2 and H_2O were omitted from the composition matrix because they can always be balanced by quartz, which is present as a nearly pure phase in all assemblages, and H_2O , which is presumed to have been present in the metamorphic fluid.

No incompatibilities were found between St assemblages (Grt, Bt, St, Ms, Pl, Ilm, \pm Chl; abbreviations after Kretz 1983) with normal ferrian ilmenite and St-Ky assemblages (Grt, Bt, St, Ms, Pl, Ilm, Ky) when they were compared by SVD. Because no mass-balance relationship exists between St and St-Ky assemblages, they must be related at least in part by a difference in bulk composition; however, one gains no information about the compositional relation between samples with different assemblages from the lack of mass balance. Incompatibilities were found where the St assemblage contains rutile-ilmenite intergrowths (Table 2, 3). Even though the rutile-ilmenite intergrowths probably were not part of the equilibrium assemblage, examination of incompatibilities involving them helps to elucidate the relationship between samples with St and St-Ky assemblages.

SVD analysis of HV2 (St assemblage with Rt-Ilm) and HV106 (St-Ky assemblage; see Table 5) yields 33 incompatibilities. A sample mass-balance relation that produces significant kyanite is:



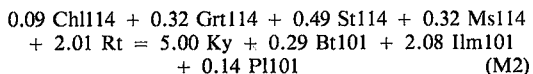
[For notation, see Lang & Rice 1985a; mineral abbreviations from Kretz (1983) are followed by the sample number without the HV prefix.] The net mass-balance relation, calculated by separating the Rt-Ilm intergrowth in HV2 into pure ilmenite and pure rutile and allowing similar Bt, Grt, etc., on either side to cancel to the extent possible, is of the form:



SVD analysis of other pairs of St assemblages with Rt-Ilm and St-Ky assemblages yields similar mass-balance relationships. Essentially the same net mass-balance relationship results if a St sample is compared with a St-Ky sample by SVD, but Rt-Ilm is eliminated and pure Rt and nearly pure ilmenite from the St-Ky sample are allowed to appear on either side of the mass-balance relation.

It was previously mentioned that some St and

some St-Ky assemblages contain chlorite that appears to have been part of the equilibrium assemblage at the peak of metamorphism. Comparison of St assemblages with equilibrium chlorite (e.g., HV114 with normal ferrian ilmenite) with St-Ky assemblages (e.g., HV101) by SVD did not yield mass-balance incompatibilities. Mass-balance relations such as the following:



resulted only if rutile was allowed to appear on the left-hand side (St assemblage). In addition to the AFM silicate relation describing the breakdown of $\text{St} + \text{Ms} \pm \text{Grt} \pm \text{Chl}$ to $\text{Ky} + \text{Bt} \pm \text{Grt}$ that would be expected to relate St to St-Ky assemblages, the net mass-balance relation in each of these examples involves a substantial amount of rutile (or excess TiO_2) on the left-hand side (St assemblage) and a similar amount of ilmenite on the right-hand side (St-Ky assemblage). This is inconsistent with the respective modes of St assemblages, which generally lack rutile, and St-Ky assemblages, which contain rutile, as will be discussed. It should be noted that muscovite is a minor participant in any of the above mass-balance relations, so that the possibility of late re-equilibration of muscovite does not present a serious problem.

INTERPRETATION

It appears from the algebraic analysis that there are no significant mass-balance incompatibilities between the St and St-Ky assemblages from the Hunt Valley Mall exposure. The only incompatibilities that were found require that the Rt-Ilm (Rt-Hem) intergrowths were part of the equilibrium assemblage, which is considered unlikely (Rumble 1976, pers. comm., 1990), or that rutile is an essential part of the St assemblage. Although a few separate grains of rutile have been found in one or two St samples, rutile is much more abundant in St-Ky assemblages. Mass balance between the St and St-Ky assemblages at Hunt Valley Mall, therefore, cannot be established.

Lack of a mass-balance relation indicates that the St and St-Ky assemblages are related at least in part by a difference in bulk composition. The nature of the critical difference in bulk composition is suggested by the incompatibilities that were found by allowing rutile to appear on either side of the mass balance (M1 net mass balance and M2). As staurolite reacts to form kyanite, some Fe-rich phase is required on the right-hand side (St-Ky

assemblage) to take up the Fe released. The requirement to balance K and Al apparently means that excess garnet and biotite on the right-hand side of the reaction cannot account for all the Fe. If pyrrhotite (present in most St-Ky samples) is presumed to be unable to participate in silicate reactions (Tracy & Robinson 1988), there is no other Fe-rich phase in the St-Ky assemblage except ilmenite. The presence of ilmenite on the right-hand side (St-Ky assemblage) requires rutile (or some other Ti-bearing phase) to be on the left (St assemblage), which is not consistent with sample modes. The mass balances that have been examined, therefore, seem to indicate that FeO cannot be balanced between the St and St-Ky assemblages and that the assemblages differ at least in part because of different effective FeO contents (also suggested by Fig. 7C). The fact that sulfide in the St-Ky assemblage ties up some of its Fe may account for some of this difference in effective bulk-composition.

The absence of a mass-balance relationship, which indicates a difference in bulk composition, does not exclude the possibility that the St and St-Ky assemblages were also related by a difference in intensive parameters (Greenwood 1967). Because significant differences in temperature and total pressure have been eliminated, variation in $\mu(\text{H}_2\text{O})$ [or $X(\text{H}_2\text{O})$] in the metamorphic fluid phase, suggested by the projection of Figure 7C, is the most likely intensive variable to influence a change from staurolite- to kyanite-bearing pelitic assemblages. Figure 8 shows the breakdown of end-member staurolite + quartz to garnet + kyanite + H_2O (metastable in the sillimanite field) at different values of $X(\text{H}_2\text{O})$ [calculated using GEØ-CALC (Brown *et al.* 1988) with Berman's August 1990 data set, ideal mixing in the fluid phase (pers. comm., 1990)]. Phase relations among the aluminosilicates, and the estimated temperature and total pressure of metamorphism (star) are shown for reference. Rocks metamorphosed in the presence of H_2O -rich fluids [at a $X(\text{H}_2\text{O})$ of 1.0 or 0.8] at the estimated T and P would contain the reactant assemblage Staurolite + Quartz (St assemblage). Rocks metamorphosed at the estimated T and P in the presence of H_2O -poor fluids [at a $X(\text{H}_2\text{O})$ of 0.4 or 0.5] would contain the product assemblage Garnet + Kyanite (St-Ky assemblage; consistent with Fig. 7C). The data for staurolite are provisional, *i.e.*, there are substantial problems with thermodynamic data and mixing models for staurolite (*cf.* Pigage & Greenwood 1982, Holdaway *et al.* 1988), so that the exact position of this equilibrium at any given value of $X(\text{H}_2\text{O})$ is questionable. The discussion of relative values of $X(\text{H}_2\text{O})$ is valid regardless of the exact

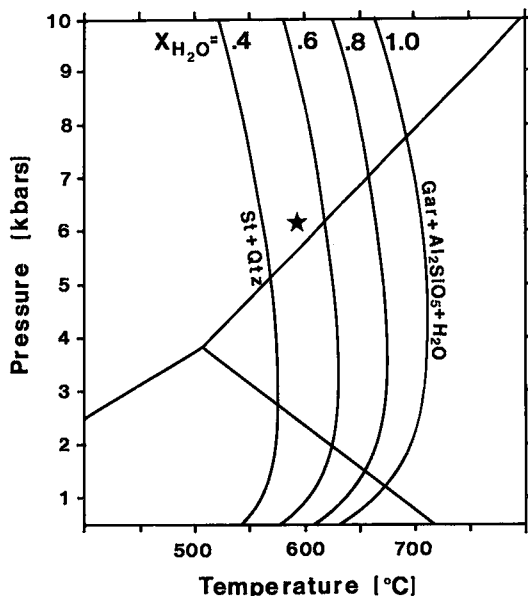


FIG. 8. GEØ-CALC P-T diagram (Brown *et al.* 1988, 1989) showing the equilibrium: Staurolite + Quartz = Almandine + Kyanite + H_2O (metastable in the sillimanite and andalusite fields) at different values of $X(\text{H}_2\text{O})$. Al_2SiO_5 phase relations are shown for reference, and the estimated temperature and total pressure of equilibration of Hunt Valley Mall samples is indicated by a star.

position of the equilibrium.

To get a provisional value for $X(\text{H}_2\text{O})$ in St-Ky assemblages, a Temperature - $X(\text{CO}_2)$ diagram was calculated using GEØ-CALC - TWEEQU (Brown *et al.* 1989, Berman 1991). The T - $X(\text{CO}_2)$ diagram with staurolite and muscovite included for St-Ky assemblage (MD22) is shown in Figure 9 (this diagram is consistent with Fig. 8, but includes more reactions that involve muscovite as well as staurolite). A very tight cluster of intersections occurs in the vicinity of 600°C and a $X(\text{CO}_2)$ of 0.5 [$X(\text{H}_2\text{O}) = 0.5$] for this sample, which is not strongly affected by re-equilibration of muscovite. The value of $X(\text{H}_2\text{O}) = 0.5$ is provisional because of uncertainties concerning the staurolite data. Reactions among paragonite (in muscovite), albite (in plagioclase) and kyanite in the Na system give a tight intersection at a similar value of $X(\text{H}_2\text{O})$. This suggests that the estimate of $X(\text{H}_2\text{O})$ based on the staurolite reactions may be reliable. It is not possible to obtain a reliable estimate of $X(\text{H}_2\text{O})$ for St assemblages because, in the absence of kyanite, most T- and $X(\text{H}_2\text{O})$ -sensitive equilibria involve muscovite or plagioclase, which causes widely scattered intersections that have already been discussed.

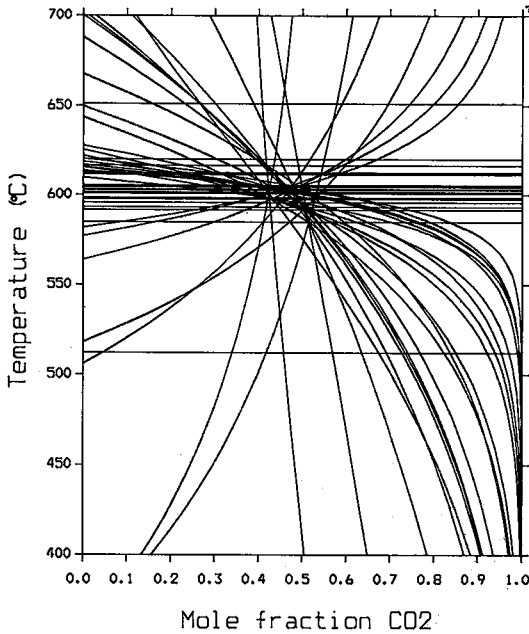


FIG. 9. GEØ-CALC T-X (CO₂) diagram at 6500 bars (Brown *et al.* 1988, 1989) showing all equilibria (stable and metastable) in the system K₂O-CaO-FeO-MgO-SiO₂-Al₂O₃-TiO₂ among mineral components in St-Ky sample MD22 including muscovite and staurolite. Equilibria are unlabeled for clarity. There is a very tight cluster of intersections among equilibria at approximately 600°C at X(CO₂) = 0.5 [X(H₂O) = 0.5].

The difference in oxide-sulfide assemblage in the St and St-Ky assemblages suggests that $f(O_2)$ and $f(S_2)$ in the metamorphic fluid may have varied in addition to $f(H_2O)$ and bulk composition. The log $f(O_2)$ versus log $f(S_2)$ diagram in Figure 10 (at 700°C and 6 kbars, after Tracy & Robinson 1988) shows that ilmenite and magnetite (common in the St assemblage) can coexist without graphite in the shaded region. In the simple system, ilmenite, rutile and pyrrhotite (common in the St-Ky assemblage) can coexist without graphite only along the short interval indicated by the heavy line. Thus, the St assemblage, which commonly contains ferrian ilmenite and magnetite (assuming that the rutile-ilmenite intergrowths resulted from supergene alteration), apparently equilibrated at similar $f(O_2)$, but lower $f(S_2)$ than the St-Ky assemblage, which commonly contains ilmenite, rutile and pyrrhotite.

CONCLUSIONS

(1) St assemblages (staurolite, garnet, biotite, quartz, muscovite, plagioclase, ilmenite and mag-

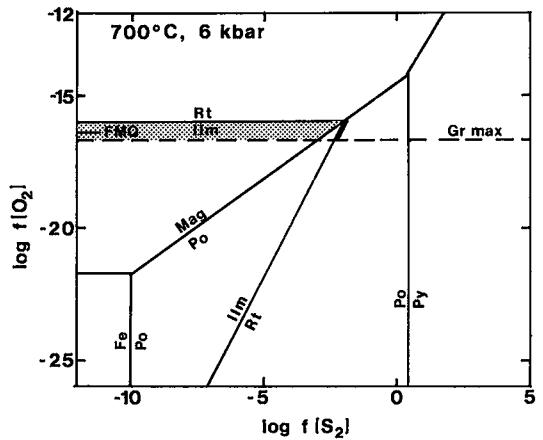


FIG. 10. A log $f(O_2)$ versus log $f(S_2)$ diagram for iron-titanium oxides and sulfides at 700°C and 6 kilobars (after Tracy & Robinson 1988). The short, heavy-line segment indicates the region in which ilmenite, rutile and pyrrhotite (common in the St-Ky assemblage) can coexist without graphite. The shading indicates the region in which ilmenite and magnetite (common in the St assemblage) can coexist without graphite. (FMQ: fayalite - magnetite - quartz buffer, Mag: magnetite, Po: pyrrhotite, Fe: iron, Ilm: ilmenite, Rt: rutile, Py: pyrite, Gr: graphite).

netite) and St-Ky assemblages (kyanite, staurolite, garnet, biotite, quartz, muscovite, plagioclase, ilmenite, rutile and pyrrhotite) from the Hunt Valley Mall exposure equilibrated at the same temperature and total pressure (approximately 590°C and 6.1 kilobar).

(2) Textures indicate that, although most of the growth of porphyroblasts occurred during D2 deformation, staurolite and garnet in some St assemblages crystallized or recrystallized after deformation. Postkinematic plagioclase porphyroblasts, which are particularly abundant in St assemblages, may have resulted from metasomatism.

(3) Although phase volumes of St assemblages and St-Ky assemblages appear to cross in AFM-Mn space, a mass-balance relationship was not confirmed by SVD analysis.

(4) The H₂O-FeO-MgO projection from average staurolite is consistent with equilibration of St assemblages at higher X(H₂O) than St-Ky assemblages.

(5) SVD shows no incompatibilities between St and St-Ky assemblages, indicating that these assemblages are related at least in part by differences in effective bulk composition, possibly FeO content.

(6) Differences in X(H₂O), which have not yet been quantified, may also have been significant in

controlling the variation in silicate mineral assemblage. A preliminary estimate of $X(\text{H}_2\text{O})$ equal to 0.5 for equilibration of St-Ky assemblages is based on staurolite and paragonite equilibria. St assemblages may have equilibrated at higher values of $X(\text{H}_2\text{O})$, as indicated in Figure 7C.

(7) Differences in oxide-sulfide assemblage between St and St-Ky assemblages indicate that St assemblages equilibrated at a similar value of $f(\text{O}_2)$, but at lower $f(\text{S}_2)$, than St-Ky assemblages.

ACKNOWLEDGEMENTS

I thank Hugh Greenwood for encouraging me and other petrologists to think quantitatively about metamorphic rocks and for providing some of the tools that are necessary for doing so. I also thank Rob Berman for providing a constructive review of the manuscript, up-to-date thermodynamic datasets, and consultation on the intricacies of GEØ-CALC; Howard Day for a constructive review, especially of the section on algebraic analysis; and George Fisher for providing the SVD programs. I thank Pam Hall for assistance in interpreting the textures, Todd Solberg for assistance with the electron microprobe, and Bill Grady for SEM photographs and analysis. This research was supported by a Faculty Senate Research Grant from West Virginia University and National Science Foundation Grant EAR-871034.

REFERENCES

- ALBEE, A.L. & RAY, L. (1970): Correction factors for electron probe microanalysis of silicates, oxides, carbonates, phosphates and sulfates. *Anal. Chem.* **42**, 1408-1414.
- BELL, T.H. & RUBENACH, M.J. (1983): Sequential porphyroblast growth and crenulation cleavage development during progressive metamorphism. *Tectonophys.* **92**, 171-194.
- BENCE, A.E. & ALBEE, A.L. (1968): Empirical correction factors for the electron microanalysis of silicates and oxides. *J. Geol.* **76**, 382-403.
- BERMAN, R.G. (1988): Internally-consistent thermodynamic data for minerals in the system $\text{Na}_2\text{O}-\text{K}_2\text{O}-\text{CaO}-\text{MgO}-\text{FeO}-\text{Fe}_2\text{O}_3-\text{Al}_2\text{O}_3-\text{SiO}_2-\text{TiO}_2-\text{H}_2\text{O}-\text{CO}_2$. *J. Petrol.* **29**, 445-522.
- _____ (1990): Mixing properties of Ca-Mg-Fe-Mn garnets. *Am. Mineral.* **75**, 328-344.
- _____ (1991): Thermobarometry using multi-equilibrium calculations: a new technique, with applications. *Can. Mineral.* **29**, 833-855.
- BROWN, T.H., BERMAN, R.G. & PERKINS, E.H. (1988): GEØ-CALC: software package for calculation and display of pressure - temperature - composition phase diagrams using an IBM or compatible personal computer. *Comput. Geosci.* **14**, 279-289.
- _____, _____ & _____ (1989): PTA-SYSTEM: a GEØ-CALC software package for the calculation and display of activity - temperature - pressure phase diagrams. *Am. Mineral.* **74**, 485-487.
- CHATTERJEE, N.D. & FROESE, E. (1975): A thermodynamic study of the pseudobinary join muscovite - paragonite in the system $\text{KAlSi}_3\text{O}_8-\text{NaAlSi}_3\text{O}_8-\text{Al}_2\text{O}_3-\text{SiO}_2-\text{H}_2\text{O}$. *Am. Mineral.* **60**, 985-993.
- CROWLEY, W.P., REINHARDT, J. & CLEAVES, E.T. (1976): Geologic map of Baltimore County and City. *Maryland Geol. Surv.*
- FISHER, G.W. (1988): Matrix analysis of metamorphic assemblages and reactions. *Geol. Soc. Am., Abstr. Programs* **20**, A159-160.
- _____ (1989): Matrix analysis of metamorphic mineral assemblages and reactions. *Contrib. Mineral. Petrol.* **102**, 69-77.
- _____, HIGGINS, M.W. & ZIETZ, I. (1979): Geological interpretations of aeromagnetic maps of the crystalline rocks in the Appalachians, northern Virginia to New Jersey. *Maryland Geol. Surv., Rep. Invest.* **32**.
- FLETCHER, C.J.N. & GREENWOOD, H.J. (1979): Metamorphism and structure of Penfold Creek area, near Quesnel Lake, British Columbia. *J. Petrol.* **20**, 743-794.
- FUHRMAN, M.L. & LINDSLEY, D.H. (1988): Ternary-feldspar modeling and thermometry. *Am. Mineral.* **73**, 201-215.
- GHEHT, E.D. (1975): Temperature, pressure and mixed-volatile equilibria attending metamorphism of staurolite-kyanite-bearing assemblages, Esplanade Range, British Columbia. *Geol. Soc. Am. Bull.* **86**, 1654-1660.
- _____ & GORDON, T.M. (1990): Al_2SiO_5 and TiO_2 activity in algebraically underdetermined metamorphic systems - constraints on metamorphic pressures. *Geol. Assoc. Can. - Mineral. Assoc. Can., Program Abstr.* **15**, A46.
- GIARAMITA, M.J. & DAY, H.W. (1989): Buffering of H_2O in staurolite - aluminum silicate - biotite - garnet - chlorite assemblages. *Geol. Soc. Am., Abstr. Programs* **21**, A238.
- GREENWOOD, H.J. (1967): The N-dimensional tie-line problem. *Geochim. Cosmochim. Acta* **31**, 465-490.

- _____ (1968): Matrix methods and the phase rule in petrology. *XXIII Intern. Geol. Congress* **6**, 267-279.
- _____ (1975): Thermodynamically valid projections of extensive phase relationships. *Am. Mineral.* **60**, 1-8.
- HALL, P.S. (1988): *Deformation and Metamorphism of the Aluminous Schist Member of the Setters Formation, Cockeysville, Maryland*. M.S. thesis, West Virginia Univ., Morgantown, West Virginia.
- HODGES, K.V. & MCKENNA, L.W. (1987): Realistic propagation of uncertainties in geologic thermobarometry. *Am. Mineral.* **72**, 671-680.
- HOLDAWAY, M.J. (1971): Stability of andalusite and the aluminosilicate phase diagram. *Am. J. Sci.* **271**, 97-131.
- _____, DUTROW, B.L. & HINTON, R.W. (1988): Devonian and Carboniferous metamorphism in west-central Maine: the muscovite - almandine geobarometer and the staurolite problem revisited. *Am. Mineral.* **73**, 20-47.
- KRETZ, R. (1983): Symbols for rock-forming minerals. *Am. Mineral.* **68**, 277-279.
- LANG, H.M. & RICE, J.M. (1985a): Regression modelling of metamorphic reactions in metapelites, Snow Peak, northern Idaho. *J. Petrol.* **26**, 857-887.
- _____ & _____ (1985b): Geothermometry, geobarometry, and T-X(Fe-Mg) relations in metapelites, Snow Peak, northern Idaho. *J. Petrol.* **76**, 889-924.
- McMULLIN, D.W.A. & BERMAN, R.G. (1990): Calibration of SGAM barometry for pelitic schists using data from phase equilibrium experiments and natural assemblages. *Geol. Assoc. Can. - Mineral. Assoc. Can., Program Abstr.* **15**, A88.
- _____ & _____ (1991): Calibration of the SGAM thermobarometer for pelitic rocks using data from phase equilibrium experiments and natural assemblages. *Can. Mineral.* **29**, 889-908.
- MULLER, P.D., CANDELA, P.A. & WYLIE, A.G. (1989): Liberty Complex; polygenetic mélange in the central Maryland Piedmont. *Geol. Soc. Am., Spec. Pap.* **228**, 113-134.
- _____ & CHAPIN, D.A. (1984): Tectonic evolution of the Baltimore Gneiss anticlines, Maryland. *Geol. Soc. Am., Spec. Pap.* **194**, 127-148.
- PIGAGE, L.C. (1976): Metamorphism of the Settler Schist, southwest of Yale, British Columbia. *Can. J. Earth Sci.* **13**, 405-421.
- _____ (1982): Linear regression analysis of sillimanite-forming reactions at Azure Lake, British Columbia. *Can. Mineral.* **20**, 349-378.
- _____ & GREENWOOD, H.J. (1982): Internally consistent estimates of pressure and temperature: the staurolite problem. *Am. J. Sci.* **282**, 943-969.
- RUMBLE, D., III (1976): Oxide minerals in metamorphic rocks. In *Oxide Minerals* (D. Rumble, III, ed.). *Rev. Mineral.* **3**, R1-24.
- _____ (1978): Mineralogy, petrology and oxygen isotopic geochemistry of the Clough Formation, Black Mountain, western New Hampshire, USA. *J. Petrol.* **19**, 317-340.
- SINHA, A.K. (1988): Granites and gabbros - a field excursion through the Maryland Piedmont. V.M. Goldschmidt Conf., Baltimore, Maryland.
- SOLBERG, T.N. & SPEER, J.A. (1982): QALL, A 16-element analytical scheme for efficient petrologic work on an automated ARL-SEM-Q: application to mica reference samples. In *Microbeam Analysis* (K.F.J. Heinrich, ed.). San Francisco Press, San Francisco, California (422-426).
- SPEAR, F.S. (1988): Thermodynamic projection and extrapolation of high-variance mineral assemblages. *Contrib. Mineral. Petrol.* **98**, 346-351.
- _____ & CHENEY, J.T. (1989): A petrogenetic grid for pelitic schists in the system SiO₂-Al₂O₃-FeO-MgO-K₂O-H₂O. *Contrib. Mineral. Petrol.* **101**, 149-164.
- _____, FERRY, J.M. & RUMBLE, D., III (1982): Analytical formulation of phase equilibria: the Gibbs method. In *Characterization of Metamorphism through Mineral Equilibria* (J.M. Ferry, ed.). *Rev. Mineral.* **10**, 105-152.
- THOMPSON, J.B., Jr. (1957): The graphical analysis of mineral assemblages in pelitic schists. *Am. Mineral.* **42**, 842-858.
- TRACY, R.J. & ROBINSON, P. (1988): Silicate - sulfide - oxide - fluid reactions in granulite-grade pelitic rocks, central Massachusetts. *Am. J. Sci.* **288-A**, 45-74.

Received December 7, 1990, revised manuscript accepted June 28, 1991.